PROCEEDINGS OF SCIENCE

Compton Scattering and the Nucleon Polarizabilities

Evangeline J. Downie[*†]
The George Washington University
E-mail: edownie@gwu.edul

The polarizabilities of the proton are fundamental quantities which describe the structure and response of the proton. They are best accessed via Compton scattering. At the MAinzer Microtoron (MAMI), the MAMI electron beam is converted to a quasi-mono-energetic tagged photon beam, with options to produce unpolarized, circularly- or linearly-polarized photons. Over the past few years, this photon beam has been employed with a variety of targets to allow access to scalar and spin polarizabilities of the proton and neutron. The experiments make use of the large-solid-angle coverage of the Crystal Ball and TAPS detector system to suppress the many large-cross-section background reactions while allowing a wide kinematic coverage. We will review the experimental program, and show the latest results on the scalar polarizabilites of the proton.

The 9th International workshop on Chiral Dynamics
17-21 September 2018
Durham, NC, USA

*Speaker.
†On behalf of the A2 Collaboration

PoS(CD2018)023

1. Introduction

In 1923, Arthur Holly Compton published his description of the effect which came to be known as Compton scattering [1]. This work was revolutionary, as it required the use of quantization and relativity. It provided evidence of the particle-like nature of the photon. As such, Compton was awarded the 1927 Nobel Prize for Physics, “for his discovery of the effect named after him.” More than ninety years later, we are still studying Compton scattering, and using Compton scattering to study other phenomena. The initial Compton scattering studies focused on scattering photons from electrons, but, later on, Compton scattering became a tool to study the properties of nucleons and nuclei. As the photon scatter is a precise process in QED, it is a very clean tool with which to study such complex objects, offering a far simpler probe than strong-force interactions. However, QED processes have low probability, and thus Compton scattering has a much smaller cross section compared to the strong-force background processes with which it competes. In order to examine polarized Compton scattering, from which one can draw even more detailed conclusions about the structure and dynamics of nucleons, one needs to use “dirty” targets - composite materials with complicated cooling and polarizing infrastructures. There is also very little to cut on in the data: at very low energies, the recoiling nucleon does not make it out of even the simplest of targets, leaving only the scattered photon energy and angle for the data analysis.

Despite these complications, Compton scattering, in both polarized and unpolarized measurements, is the most commonly used mechanism to investigate the nucleon polarizabilities. These are fundamental constants which describe nucleon structure and dynamics. At the lowest order, one speaks of the electric and magnetic scalar polarizabilies of the proton. The electric polarizability, α, describes the “stretchability” of the proton, the response of the pion cloud to an applied electric field, where the induced dipole field ($\vec{d_{ind}}$), is proportional to the applied field ($\vec{E}$), and α is the constant of proportionality

$$\vec{d_{ind}} = 4\pi\alpha\vec{E} \tag{1.1}$$

The magnetic polarizability (β) is analagous, with $\vec{B}$, the applied magnetic field, and $\vec{m_{ind}}$ the induced field.

$$\vec{m_{ind}} = 4\pi\beta\vec{B} \tag{1.2}$$

However, the response of the nucleon constitutents to a magnetic field is more complex than that to an electric field. The charged components of the nucleon tend to rotate against the direction of the applied field in a diamagnetic response, while those constitutents with spin align with the field in a paramagnetic response. This mixed reaction leads to β being far smaller that α.

2. Why measure the polarizabilities?

The polarizabiliites are more than simply fundamental constants, they play a role in many areas of hadronic physics. They give major contributions to the susceptibility of nuclei and neutron stars [2]. They contribute the largest uncertainity in the electromagnetic component of the proton-neutron mass difference [3]. They are the largest source of uncertainty in the proton radius extractions from spectroscopy, and were even purported to explain the proton radius puzzle completely (although that is not generally accepted) [4, 5, 6].

The polarizabilities are extracted from Compton scattering cross sections by fitting with theories from a variety of backgrounds: typically dispersion relations [7], heavy baryon chiral perturbation theory [9], and chiral effective field theories [8, 10]. Despite the importance of the polarizabilities, there is insufficient precision in the current database to fully constrain their extraction. In 2009, a prediction of Chiral Effective Field Theory [10] appeared to describe the world data as well as a dispersion-relation-based fit [11], while giving a magnetic polarizability twice as large. In response to this uncertainty, a group of theorists and an experimentalist collaborated to produce a curated Compton scattering world data set, excluding inconsistent points, and then fit these data to extract nucleon polarizabilities [12]. This extraction was later updated [9]. This very careful analysis gave:

$$\alpha = [10.65 \pm 0.35\,(stat.) \pm 0.2\,(Baldin) \pm 0.3\,(theory)]x10^{-4}fm^3 \tag{2.1}$$

$$\beta = [3.15 \mp 0.35\,(stat.) \pm 0.2\,(Baldin) \mp 0.3\,(theory)]x10^{-4}fm^3 \tag{2.2}$$

The Particle Data Group took note, as their values of

$$\alpha = [12.0 \pm 0.6]x10^{-4}fm^3 \tag{2.3}$$

$$\beta = [1.9 \pm 0.5]x10^{-4}fm^3 \tag{2.4}$$

changed to

$$\alpha = [11.2 \pm 0.4]x10^{-4}fm^3 \tag{2.5}$$

$$\beta = [2.5 \pm 0.4]x10^{-4}fm^3 \tag{2.6}$$

between the 2012 and 2013 update [13] with no new experimental data, simply due to the curation and reanalysis of the existing world data set. This indicates very clearly that new, high-quality data are needed to constrain the extraction of these constants, which are of interest for objects from the scale of neutron stars, all the way down to to the proton radius.

3. Measurement of the scalar polarizabilities

Until the recent A2 collaboration measurement campaign at MAMI, and the efforts of the Compton collaboration at HIGS, the world's most comprehensive Compton scattering data set came from the TAPS experiment at MAMI [14]. This employed the TAPS detector, in six segmented walls (Fig. 1), to produce cross sections for photon energies from 60 to 180 MeV, at polar angles from 59° to 155°. The data significantly improved the available world data set, as can be seen in Fig. 2. The polarizability results were extracted using dispersion relations calculated by L'vov [15].

As the extraction from such unpolarized cross-section data is always a joint extraction of linear combinations of α and β, the absolute uncertainties of α and β are similar in size, resulting in a much larger relative error on the far smaller β. In 2013, Krupina and Pascalutsa [8] suggested a modification to this traditional extraction methodology. If one measures the photon asymmetry, Σ_3 (the difference in cross section for photons polarized parallel and perpendicular to the reaction plane, divided by the sum) at certain angles, the influence of α is kinematically suppressed, and one has more direct access to β.

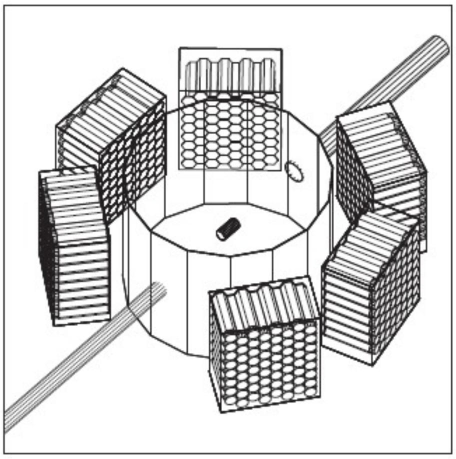

Figure 1: TAPS experimental setup of Olmos de Lyon *et al.* [14].

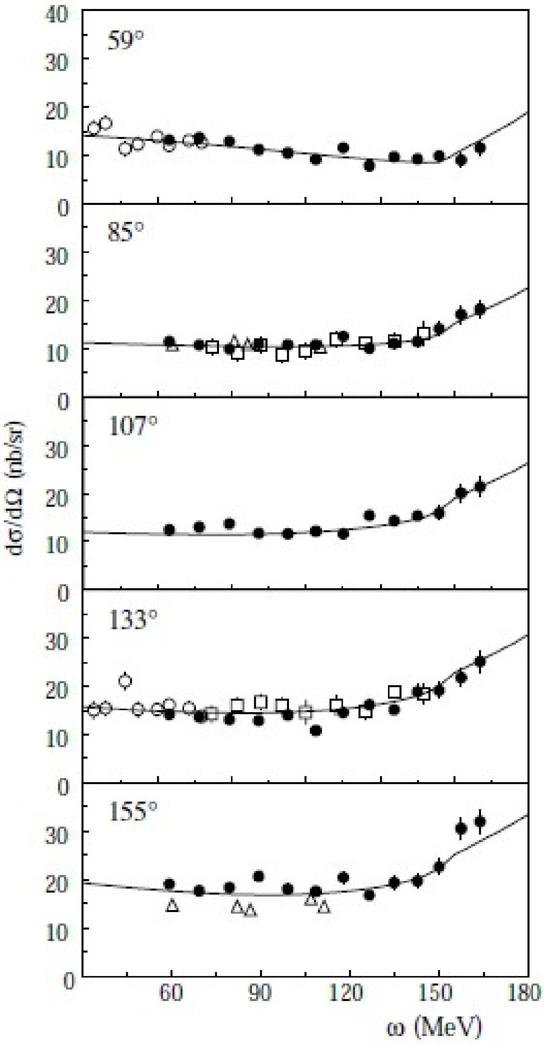

Figure 2: Results from [14] (closed circles), plotted with: triangles [16]; open circles [17]; squares [18]; The solid line shows the calculation of the dispersion relation approach using the π-production multipoles of [19].

4. The A2 experiment

In 2012 it was proposed to make such a measurement within the A2 experimental hall of the MAMI accelerator, in Mainz, Germany, using the Crystal Ball and TAPS setup [20]. The experiment recieved an A-rating from the PAC, and requested 750 hours of data taking.

MAMI produces, through a series of three cascaded Racetrack Microtrons and the world's only Harmonic Double Sided Microtron [21], an electron beam of up to 100 μA with up to 85% beam polarization, variable energy up to 1604 MeV and 100% duty factor.

The A2 photon beam is derived from the production of Bremsstrahlung photons during the passage of the MAMI electron beam through a thin radiator. The resulting photons can be circularly polarized, with the application of a polarized electron beam, or linearly polarized, in the case of a crystalline radiator. The degree of polarization achieved is dependent on the energy of the incident photon beam (E_0) and the energy range of interest, but currently peaks at ∼75% for linear polarization and ∼85% for circular polarization.

The Glasgow Photon Tagger (Fig, 3) provides energy tagging of the photons by detecting the post-radiating electrons and can determine the photon energy with a resolution of 1 to 4 MeV, depending on the incident beam energy, with a single-counter time resolution $\sigma_t = 0.117$ ns [22]. Each counter can operate reliably to a rate of ∼1 MHz, giving a photon flux of $2.5 \cdot 10^5$ photons per MeV. Photons can be tagged in a continuous momentum range from 4.7 to 93.0% of E_0.

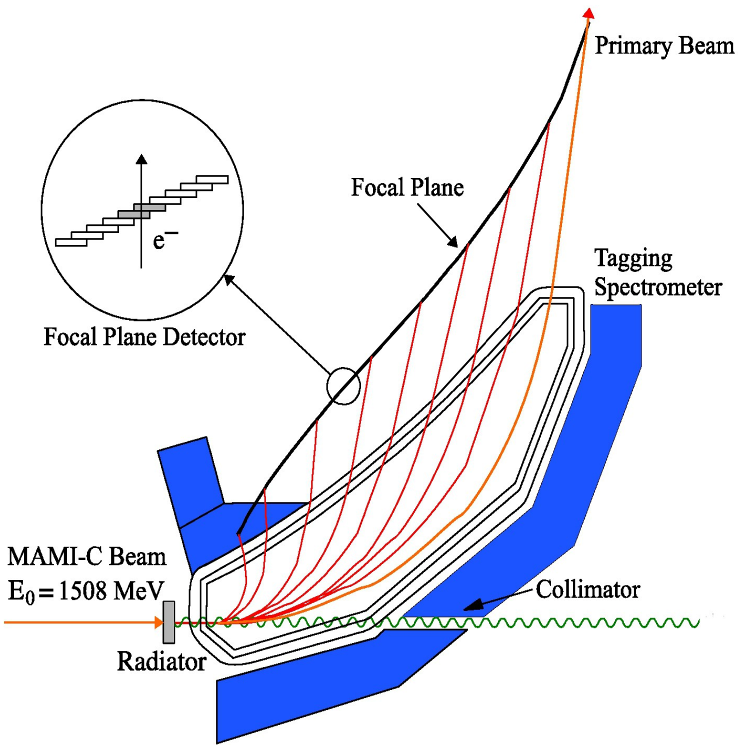

Figure 3: A diagram of the Glasgow-Mainz Photon Tagging spectrometer.

The tagged photon beam impinges on a standard cryogenic liquid hydrogen target, which can be set to have a variety of lengths from 3 to 10 cm. The central detector system, surrounding the liquid hydrogen target, consists of the Crystal Ball calorimeter combined with a barrel of scintillation counters for particle identification and two coaxial multi-wire proportional counters for charged particle tracking. This central system provides position, energy and timing information for both charged and neutral particles in the region between 21° and 159° in the polar angle (θ) and over almost the full azimuthal (ϕ) range. At forward angles, less than 21°, reaction products are detected in the TAPS forward wall. The full, almost hermetic, detector system is shown schematically in Fig. 4.

The largest challenge in carrying out a measurement of Compton scattering is the low cross section, meaning experiments need to maximize luminosity and detector acceptance. The other major challenge to extracting a clean measurement of Compton scattering is the π^0 production background channel, which has cross sections vastly greater than those of Compton scattering. If one of the two π^0 decay photons goes undetected, π^0 production can appear to be Compton scattering. Thus to minimize pion backgrounds, it is necessary to have a large-acceptance detector in order to minimize the probability of missing one of the two decay photons. Thus the large-acceptance CB TAPS detector system is superior to the TAPS setup shown in Fig. 1.

The Crystal Ball detector is a highly segmented 672-element NaI(Tl), self triggering photon spectrometer. The CB has an energy resolution of $\Delta E/E = 0.020 \cdot E[GeV]^{0.36}$ and angular resolutions of $\sigma_\theta = 2-3^\circ$ and $\sigma_\phi = \sigma_\theta / \sin\theta$ for electromagnetic showers [23], with a large dynamic range [24]. The FPGA triggering system allows the construction of flexible and intelligent triggers for the program. For instance, once the energy is sufficient that the target proton can escape the target, one could select on two back-to-back particles, one charged, one not, thereby minimizing the π^0 background at the hardware level and allowing us to run more efficiently.

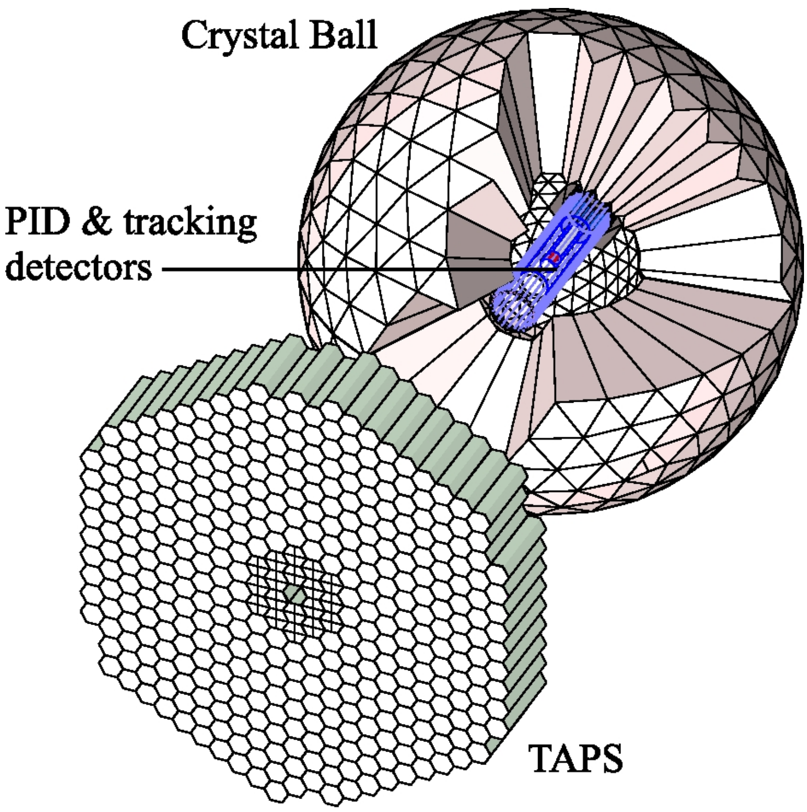

Figure 4: A diagram of the Crystal Ball detector system, showing the Crystal Ball NaI calorimeter, surrounding the liquid hydrogen target, Particle Identification Detector for charged particle identification, and two Multiwire Proportional Wire Chambers to enhance charged particle tracking. The TAPS detector forward BaF2 wall measures the reaction particles exiting the detector system at forward angles.

In order to distinguish between neutral and charged particles species detected by the CB, the system is equipped with the Particle Identification Detector (PID2), a barrel detector of twenty-four scintillators, arranged so that each PID2 scintillator subtends an angle of 15° in ϕ. By matching a hit in the PID2 with a corresponding hit in the CB, it is possible to use the locus of the $\Delta E, E$ combination to identify the charged particle species. The charged particle position resolution is enhanced by a pair of Multi-Wire Proportional Chambers with an angular resolution (rms) of $\sim 2^\circ$ in the polar emission angle θ and $\sim 2^\circ$ in the azimuthal emission angle ϕ.

The TAPS forward wall is composed of 384 BaF_2 elements. The front of every TAPS element is covered by a 5 mm thick plastic veto scintillator. The single counter time resolution is $\sigma_t = 0.2$ ns, the energy resolution can be described by $\Delta E/E = 0.018 + 0.008/E[GeV]^{0.5}$ [23]. The angular resolution in the polar angle is better than 1°. The TAPS readout was custom built for the beginning of the CB@MAMI program and is effected in such a way as to allow particle identification by Pulse Shape Analysis (PSA), Time Of Flight (TOF) and $\Delta E/E$ methods (using the energy deposit in the plastic scintillator to give ΔE). TAPS can also contribute to the new FPGA trigger system. The two inner rings of 18 BaF_2 elements have been replaced by 72 $PbWO_4$ crystals, each 20 cm in length (22 radiation lengths). The higher granularity improves the rate capability as well as the angular resolution. The crystals are operated at room temperature. The energy resolution for photons is similar to BaF_2 under these conditions [25].

MAMI has a program which spans scalar and spin polarizabilities, of both protons and neutrons, but here we will focus on the proton scalar polarizabilites.

5. Scalar polarizability results

In May 2013, three hundred hours of the allocated 750 hours of data were taken. In 2017, this first measurement of Σ_3 below pion production threshold was published [26]. It was a very challenging experiment, as the single-photon, low-threshold trigger necessary to gather the data was the most open trigger which had been used within the CB setup at MAMI. It led to new backgrounds which had not previously been observed. Thus a substantial fraction of the three hundred hours was used in investigating this background. In the end, more than 200,000 Compton scattering events were measured in an incoming photon energy range from 76 to 139 MeV, and a polar angle range of 30° to 155°. This was sufficient to demonstrate proof-of-principle that the polarizabilities could be extracted from the asymmetry, but the statistics of the experiment were insufficient to improve on the extracted value of the polarizabilities.

As the statistical limit of the experiment was also, in part, due to the maximum rate which the photon tagger could run, it was decided to postpone the remaining data-taking until after the planned upgrade of the tagger focal plane detector system. The Glasgow-Mainz Photon Tagger focal plane detector was a series of 353 overlapping scintillators, which were each angled to have a 50% overlap with each of its two neighboring scintillators. Each "channel" was formed by an AND of each neighboring pair of scintillators, giving 352 channels. Each physical scintillator was individually sized to cover the same momentum bite per channel, roughly 1cm in width, and was rate-limited to 1 MHz.

This system was replaced with 408, non-overlapping, 6x6 mm scintillating fibers made from EJ-200. These are read out by 6x6mm. SensL-SiPMs, allowing for a vast increase in rate, and thus an enhanced photon flux.

Subsequent to the Tagger focal plane renovation, 66 days of data were taken, across four beam times, giving a total of 460 hours of target-full and 300 hours of target-empty data. This enabled the collection of over one million events in an incoming photon energy range from 80 to 140 MeV, and a polar angle range of 30° to 155°.

This data is under analysis by Edoardo Mornacchi of Johannes Gutenberg Universitaet, Mainz. The quality of the data can be seen in Fig. 5, and its improvement over the asymmetry in [26] in Fig. 6. The unpolarized cross section data can be seen in Fig. 7. The final asymmetry results are shown in Fig. 8. The data analysis and systematics are being finalized and the collaboration is working with theorists on the extraction of α and β.

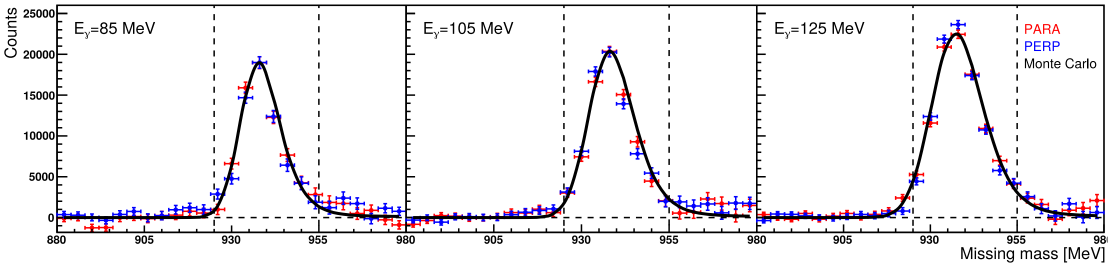

Figure 5: PRELIMINARY: The invariant mass extracted from the data separately for both polarization states (red and blue crosses) and simulation (black curve), using roughly one third of the data [27].

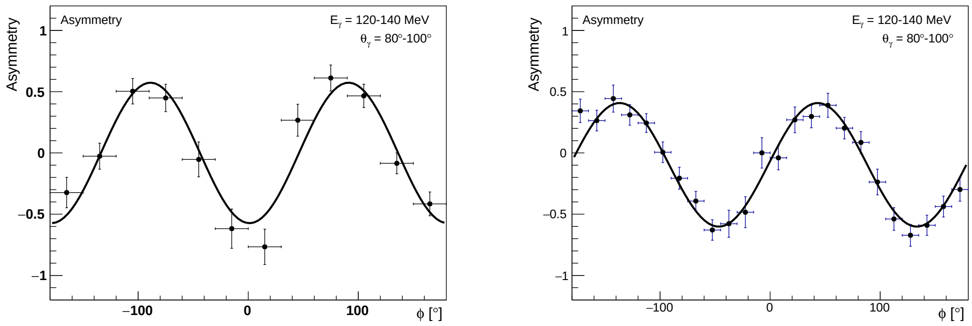

Figure 6: PRELIMINARY: Comparison between the data quality in [26] **(left)** vs. that in the new, as yet unpublished, experiment [27] **(right)**.

6. Conclusion

Compton scattering and the nucleon polarizabilities are of ongoing interest for many areas of physics. However, the available data is still insufficient to fully determine all of the scalar and spin polarizabilites. Thus there is still much work to be done at both MAMI and HIGS.

At MAMI, the proof-of-principle photon asymmetry measurement was successful, extracting both α and β [26], but in order to make a more significant extraction, more statistics are needed. In order to improve the rate capability in the A2 experimental hall, the Tagger focal plane detector was upgraded. After this upgrade, over 750 hours of data were collected, and the results look very

PoS(CD2018)023

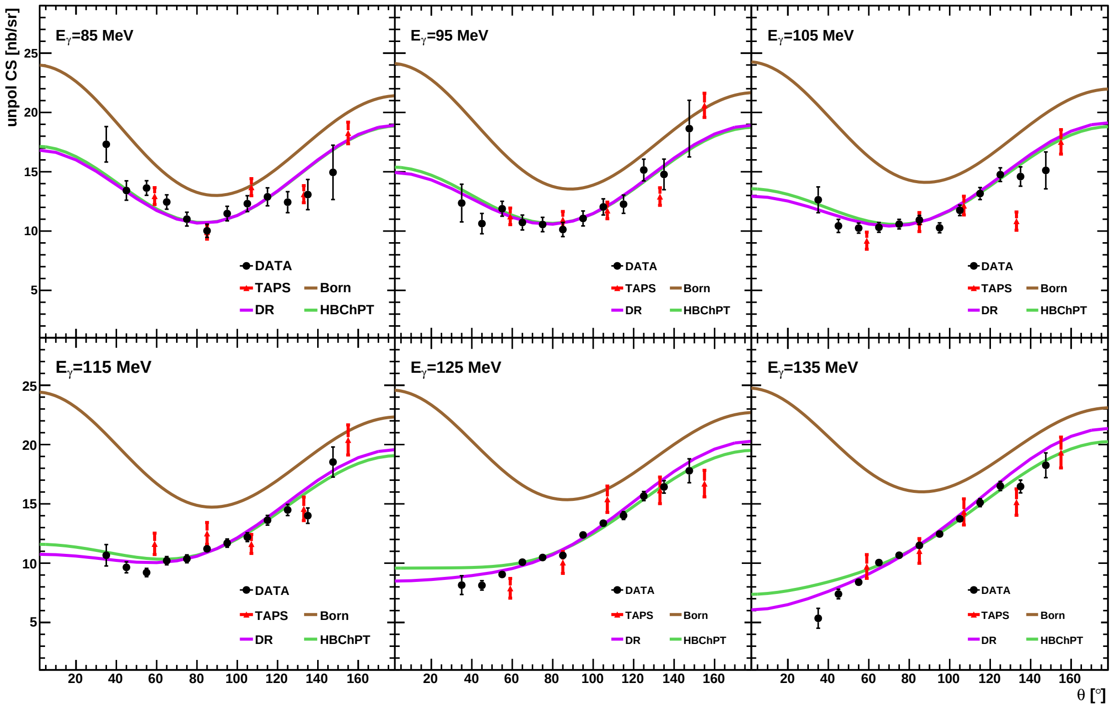

Figure 7: PRELIMINARY: The unpolarized cross section extracted from [27] (black circles), compared to that from [14] (red triangles). The brown curve shows the Born contribution; magenta shows a dispersion relation calculation with $\alpha = 10.65$, $\beta = 3.15$ [7]; and green the heavy baryon chiral perturbation theory calculation of [9], with the same polarizability values.

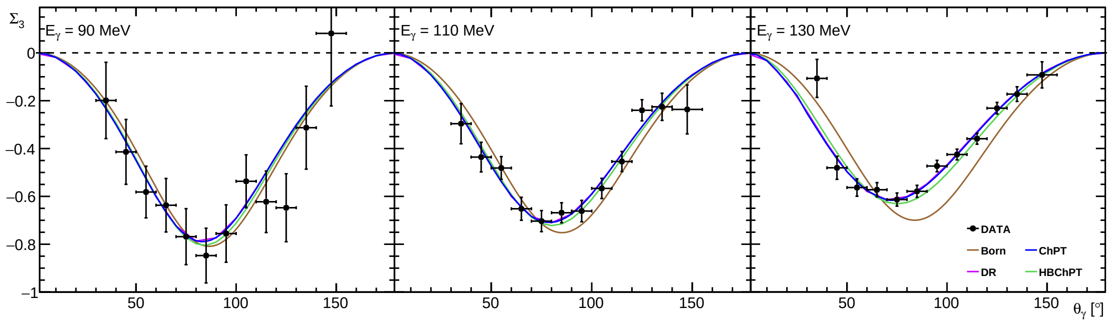

Figure 8: PRELIMINARY: The Σ_3 asymmetry extracted from [27], with curves showing the Born contribution; a dispersion relation calculation with $\alpha = 10.65$, $\beta = 3.15$ [7] (magenta); Heavy Baryon Chiral Perturbation Theory calculation of [9], with the same polarizability values (green); and ChiPT of [10] (blue).

promising. The data are under analysis by Edoardo Mornacchi [27], with support from Phillippe Martel and Judith McGovern for fitting and theoretical interpretation.

All of the extractions of polarizabilites from Compton scattering data require strong collaboration with the theorists who are developing the models used. Active collaboration to identify the most sensitive measurements, and to ensure that models are only appropriately employed is indispensable to this program.

Thanks to this close collaboration between theory and experiment, and the ever-improving accelerators and detector systems, there is a bright and very active future for Compton Scattering and the nucleon polarizabilities at both MAMI and HIGS.

Acknowledgments

This material is based upon work supported by the National Science Foundation under Grant Number PHY-1714833, and the Department of Energy under award DE-SC0016581. Thanks are due to Edoardo Mornacchi and Phillippe Martel for sharing the preliminary data, to Vahe Sokhoyan for his collaboration on the pilot experiment, and to Judith McGovern for her patient insight into the theory, and collaboration on data-fitting. Also to all the members of the A2 Collaboration whose efforts made these measurements possible.

References

[1] A. H. Compton, *A Quantum Theory of the Scattering of X-rays by Light Elements*, *Phys. Rev.* **21** (1923) 483.

[2] J. Bernabeu, T. E. O. Ericson and C. Ferro Fontan, *The Nucleon Electromagnetic Polarizabilities*, *Phys. Lett.* **49B** (1974) 381.

[3] A. Walker-Loud, C. E. Carlson and G. A. Miller, *The Electromagnetic Self-Energy Contribution to M_p - M_n and the Isovector Nucleon Magnetic Polarizability*, *Phys. Rev. Lett.* **108** (2012) 232301 [1203.0254].

[4] G. A. Miller, *Proton Polarizability Contribution: Muonic Hydrogen Lamb Shift and Elastic Scattering*, *Phys. Lett.* **B718** (2013) 1078 [1209.4667].

[5] R. Pohl, R. Gilman, G. A. Miller and K. Pachucki, *Muonic hydrogen and the proton radius puzzle*, *Annual Review of Nuclear and Particle Science* **63** (2013) 175 [https://doi.org/10.1146/annurev-nucl-102212-170627].

[6] C. E. Carlson, *The Proton Radius Puzzle*, *Prog. Part. Nucl. Phys.* **82** (2015) 59 [1502.05314].

[7] B. Pasquini, D. Drechsel and M. Vanderhaeghen, *Proton spin polarizabilities from polarized Compton scattering*, *Phys. Rev.* **C76** (2007) 015203 [0705.0282].

[8] N. Krupina and V. Pascalutsa, *Separation of proton polarizabilities with the beam asymmetry of Compton scattering*, *Phys. Rev. Lett.* **110** (2013) 262001 [1304.7404].

[9] J. A. McGovern, D. R. Phillips and H. W. Griesshammer, *Compton scattering from the proton in an effective field theory with explicit Delta degrees of freedom*, *Eur. Phys. J.* **A49** (2013) 12 [1210.4104].

[10] V. Lensky and V. Pascalutsa, *Predictive powers of chiral perturbation theory in Compton scattering off protons*, *Eur. Phys. J.* **C65** (2010) 195 [0907.0451].

[11] S. Beane, M. Malheiro, J. McGovern, D. R. Phillips and U. van Kolck, *Compton scattering on the proton, neutron, and deuteron in chiral perturbation theory to $O(Q^4)$*, Nucl.Phys. **A747** (2005) 311 [nucl-th/0403088].

[12] Griesshammer, H.W. and McGovern, J.A. and Phillips, D.R. and Feldman, G., *Using effective field theory to analyse low-energy Compton scattering data from protons and light nuclei*, Prog.Part.Nucl.Phys. **67** (2012) 841 [1203.6834].

[13] Particle Data Group collaboration, *Review of Particle Physics (RPP)*, Phys. Rev. **D86** (2012) 010001.

[14] V. Olmos de Leon, F. Wissmann, P. Achenbach, J. Ahrens, H. J. Arends, R. Beck et al., *Low-energy Compton scattering and the polarizabilities of the proton*, Eur. Phys. J. **A10** (2001) 207.

[15] A. I. L'vov, V. A. Petrun'kin and M. Schumacher, *Dispersion theory of proton Compton scattering in the first and second resonance regions*, Phys. Rev. **C55** (1997) 359.

[16] P. Baranov et al., *New experimental data on the proton electromagnetic polarizabilities*, Phys. Lett. **B52** (1974) 122.

[17] F. Federspiel, R. Eisenstein, M. Lucas, B. MacGibbon, K. Mellendorf et al., *The proton Compton effect: A measurement of the electric and magnetic polarizabilities of the proton*, Phys.Rev.Lett. **67** (1991) 1511.

[18] B. E. MacGibbon, G. Garino, M. A. Lucas, A. M. Nathan, G. Feldman and B. Dolbilkin, *Measurement of the electric and magnetic polarizabilities of the proton*, Phys. Rev. **C52** (1995) 2097 [nucl-ex/9507001].

[19] R. A. Arndt, I. I. Strakovsky and R. L. Workman, *Updated resonance photo-decay amplitudes to 2 GeV*, Phys. Rev. **C53** (1996) 430 [nucl-th/9509005].

[20] E. J. Downie, J. R. M. Annand, D. Hornidge and R. Miskimen, *Proposal to the MAMI PAC, MAMI-A2/06-2012: Measurement of the Proton Scalar Polarizabilities*, 2012.

[21] K. H. Kaiser, K. Aulenbacher, O. Chubarov, M. Dehn, H. Euteneuer, F. Hagenbuck1 et al., *The 1.5-GeV Harmonic Double-Sided Microtron at Mainz University*, Nucl.Instrum.Meth. **A593** (2008) 159.

[22] J. McGeorge, J. Kellie, J. Annand, J. Ahrens, I. Anthony, A. Clarkson et al., *Upgrade of the Glasgow photon tagging spectrometer for Mainz MAMI-C*, Eur.Phys.J. **A37** (2008) 129 [0711.3443].

[23] Crystal Ball Collaboration at MAMI, A2 Collaboration collaboration, *Measurement of the Slope Parameter alpha for the $\eta \to 3\pi^0$ decay with the Crystal Ball at MAMI-C*, Phys.Rev. **C79** (2009) 035204 [0812.1999].

[24] The Crystal Ball collaboration, *Incoherent pion photoproduction on ^{12}C*, Phys. Rev. Lett. **100** (2008) 132301 [0711.1839].

[25] R. Novotny, R. Beck, W. Doring, V. Hejny, M. Hoek, A. Hofstaetter et al., *Scintillators for photon detection at medium energies: A comparative study of BaF-2, CeF-3 and PbWO-4*, Nucl.Instrum.Meth. **A486** (2002) 131.

[26] A2 collaboration, *Determination of the scalar polarizabilities of the proton using beam asymmetry Σ_3 in Compton scattering*, Eur. Phys. J. **A53** (2017) 14 [1611.03769].

[27] E. Mornacchi and P. Martel, *Private communication of preliminary data*, 2019.